ISSN 1063-7826, Semiconductors, 2015, Vol. 49, No. 13, pp. 1718–1726. © Pleiades Publishing, Ltd., 2015.
Original Russian Text © M.I. Zavgorodnyaya, I.V. Lavrov, A.G. Fokin, 2015, published in Izvestiya vysshikh uchebnykh zavedenii. Elektronika, 2014, Vol. 109, No. 5, pp. 3–14.

MATERIALS FOR ELECTRONIC ENGINEERING

Analytical Approach to Calculating the Effective Dielectric Characteristics of Heterogeneous Textured Materials with Randomly Shaped Inclusions

M. I. Zavgorodnyaya[a], I. V. Lavrov[b]*, and A. G. Fokin[b]

[a]*National Research Nuclear University "MEPhI", Kashirskoe sh. 31, Moscow, 115409 Russia*
[b]*National Research University of Electronic Technology, Ploschad' Shokina 1, Zelenograd, Moscow, 124498 Russia*
** e-mail: iglavr@mail.ru*

Submitted March 25, 2014

Abstract—Analytical expressions for calculating the tensor of the effective permittivity of a matrix-type heterogeneous medium with inclusions of random ellipsoidal shape, which are a small deviation from the average spheroidal shape, are obtained. The orientations of the inclusions are probabilistically distributed; rotation group representations are used for their consideration. It is shown that the developed method is a generalization of the Maxwell–Garnett approximation for the given medium type. Based on this method, the frequency-induced dielectric properties of porous silicon are simulated in the range of 10^3–10^8 Hz.

Keywords: heterogeneous material, effective permittivity tensor, texture, orientation, random shape, ellipsoid, Maxwell–Garnett approximation.

DOI: 10.1134/S1063782615130163

INTRODUCTION

Heterogeneous materials, i.e., inhomogeneous materials, whose local physical characteristics are piecewise constant functions of spatial coordinates, play an important role in science and engineering. For example, porous silicon and carbon, thin polycrystalline and composite films of different functionalities find wide application in electronics. In many applications, of importance is the behavior of such materials in alternating electromagnetic fields, which is determined by the effective permittivity of such a material under the condition of smallness of the inhomogeneity scale in comparison with field-inhomogeneity parameters. This causes the stable interest of researchers in the problem of its calculation. In turn, the effective permittivity of a heterogeneous material depends not only on the dielectric properties of its components and their volume fractions, but also on structure formed by them.

Important components of the structure are the shape texture and crystallographic texture whose manifestation is anisotropy of the effective material properties. The most effective approach which can naturally take into account the material texture is associated with the introduction of a reference body. In this approach, along with the problem for the initial heterogeneous medium, a similar problem for the reference body is considered [1–5]. Then, via certain transformations and assumptions, one can come to some approximation, e.g., the generalized singular approximation [2] which has also found wide application in calculating the effective elastic moduli of heterogeneous media [3].

In [6–9], the effective dielectric characteristics of textured composites were calculated. In [6, 7], matrix axially textured composites with spheroidal isotropic [6] or spherical biaxial anisotropic [7] inclusions were considered. In [8], a method for taking the orientations of ellipsoidal isotropic inclusions into account using SO(3) group representations and allowing a fundamental advance in deriving expressions for the effective characteristics of a composite for any texture type was proposed. In [9, 10], this method was generalized to the case of anisotropic ellipsoidal inclusions provided that the principal axes of the inclusion permittivity tensors coincide with the ellipsoid axes.

The objective of this study is to derive analytical expressions for components of the effective permittivity tensor of a textured matrix composite with inclusions whose shape is random ellipsoidal and is a small deviation from the spheroidal shape. A fundamental version of consideration of the shape randomness within the ellipsoidal shape was proposed in [11]. However, its implementation requires a very resource-intensive procedure: calculations of double integrals of quantities which are themselves expressed in terms of elliptical integrals. In [12], a composite with inclusions of random spheroidal shape whose semiaxis ratio is uniformly distributed in a certain range was considered.

STATEMENT OF THE PROBLEM AND ITS SOLUTION IN THE GENERALIZED MAXWELL–GARNETT APPROXIMATION

Let us consider a statistically homogeneous sample of a two-component composite of volume V, consisting of a homogeneous isotropic matrix with ellipsoidal anisotropic inclusions immersed into it. The volume fraction d of inclusions is not high. It is assumed that the principal axes of the permittivity tensors of the inclusions coincide with the axes of the corresponding ellipsoids. Inclusions are oriented probabilistically and have a random ellipsoidal shape being a small deviation from the spheroidal shape. The inclusion shape and orientation are considered independent of each other.

Let a constant electric field $\mathbf{E_0}$ be applied to the boundary S of this sample. The medium permittivity tensor $\boldsymbol{\varepsilon}(\mathbf{r})$ is a random piecewise constant function of coordinates:

$$\boldsymbol{\varepsilon}(\mathbf{r}) = \begin{cases} \varepsilon_m \mathbf{I}, & \mathbf{r} \in V_m, \\ \boldsymbol{\varepsilon}_k, & \mathbf{r} \in V_k, \quad k = \overline{1, N}, \end{cases} \tag{1}$$

where ε_m is the permittivity of the matrix, V_m is the region occupied by the matrix, $\mathbf{I}$ is the unit tensor, $\boldsymbol{\varepsilon}_k$ and V_k are the permittivity tensor of the k-th inclusion and the region occupied by it, respectively, and N is the number of inclusions in the sample.

From electrostatic equations $\operatorname{div} \mathbf{D} = 4\pi\rho$, $\operatorname{curl} \mathbf{E} = 0$, taking into account the constitutive equation $\mathbf{D} = \boldsymbol{\varepsilon}\mathbf{E}$, we come to the boundary-value problem for the potential $\varphi(\mathbf{r})$ in a given medium ($\mathbf{E} = -\nabla\varphi$):

$$\nabla \cdot \boldsymbol{\varepsilon}(\mathbf{r}) \nabla \varphi(\mathbf{r}) = -4\pi\rho(\mathbf{r}), \quad \varphi\big|_S = -(\mathbf{E}_0 \cdot \mathbf{r}), \tag{2}$$

where $\rho(\mathbf{r})$ is the volume charge density.

The problem lies in calculating the tensor $\boldsymbol{\varepsilon}_\mathbf{e}$ of the effective permittivity of the composite, which relates the average electrical displacement and electric-field strength vectors, $\langle \mathbf{D} \rangle = \boldsymbol{\varepsilon}_\mathbf{e} \langle \mathbf{E} \rangle$. We introduce a homogeneous reference body with the same sizes, shape, and charge density distribution as those of the composite sample [1–5]. We present $\varphi(\mathbf{r})$ and $\boldsymbol{\varepsilon}(\mathbf{r})$ in the form $\varphi(\mathbf{r}) = \varphi^c(\mathbf{r}) + \varphi'(\mathbf{r})$, $\boldsymbol{\varepsilon}(\mathbf{r}) = \boldsymbol{\varepsilon}^c + \boldsymbol{\varepsilon}'(\mathbf{r})$, where index "$c$" is related to the reference body. For the reference body, a problem similar to Eq. (2) is formulated as

$$\nabla \cdot \boldsymbol{\varepsilon}^c \nabla \varphi^c(\mathbf{r}) = -4\pi\rho(\mathbf{r}), \quad \varphi^c\big|_S = -(\mathbf{E}_0 \cdot \mathbf{r}). \tag{3}$$

Subtracting Eq. (3) from Eq. (2), we obtain the boundary-value problem:

$$\nabla \cdot \boldsymbol{\varepsilon}^c \nabla \varphi'(\mathbf{r}) = -\nabla \cdot \boldsymbol{\varepsilon}'(\mathbf{r}) \nabla \varphi(\mathbf{r}), \quad \varphi'\big|_S = 0. \tag{4}$$

Introducing the Green function $G(\mathbf{r}, \mathbf{r}_1)$ of problem (4) by the conditions

$$\nabla \cdot \boldsymbol{\varepsilon}^c \nabla G(\mathbf{r}, \mathbf{r}_1) = -\delta(\mathbf{r} - \mathbf{r}_1), \quad G(\mathbf{r}, \mathbf{r}_1)\big|_{\mathbf{r}_1 \in S} = 0,$$

the solution to problem (4) at $V \to \infty$ is written in the form of the convolution [1, 2, 5]:

$$\varphi'(\mathbf{r}) = \int G(\mathbf{r}_1 - \mathbf{r}) \nabla \cdot \boldsymbol{\varepsilon}'(\mathbf{r}_1) \nabla \varphi(\mathbf{r}_1) d\mathbf{r}_1.$$

After some transformations, to calculate $\boldsymbol{\varepsilon}_\mathbf{e}$ in the generalized singular approximation [5], we obtain the expression

$$\boldsymbol{\varepsilon}_\mathbf{e} = \left\langle \boldsymbol{\varepsilon}(\mathbf{r}) \left(\mathbf{I} - \mathbf{g}\,\boldsymbol{\varepsilon}'(\mathbf{r})\right)^{-1} \right\rangle \left\langle \left(\mathbf{I} - \mathbf{g}\,\boldsymbol{\varepsilon}'(\mathbf{r})\right)^{-1} \right\rangle^{-1}, \tag{5}$$

where $\mathbf{g}$ is the tensor related to a particular inhomogeneity grain (the matrix can also be considered as consisting of individual grains) and taking a constant value within it, and its components are calculated by the formula [1, 5]

$$g_{ij} = \oint_{S'} \nabla_i G(\mathbf{r}) n_j dS,$$

where n_j is the j-th component of the external unit normal to S'. Integration is performed over the surface S' of a given inhomogeneity grain.

For a matrix medium, it is logical to take specifically a matrix as a reference medium, i.e., to accept $\boldsymbol{\varepsilon}^c = \varepsilon_m \mathbf{I}$.

In this case, the tensor components $\mathbf{g}_k$ of the ellipsoidal inclusion in its intrinsic system can be written as [1]

$$g_{ij} = -(\varepsilon_m)^{-1} L_i \delta_{ij}, \quad i, j = 1, 2, 3,$$

where L_i are the geometrical factors of the ellipsoid (a_1, a_2, a_3 are its semiaxes) [11]:

$$L_i = \frac{a_1 a_2 a_3}{2} \int_0^\infty \frac{dq}{(a_i{}^2 + q)\left[(a_1{}^2 + q)(a_2{}^2 + q)(a_3{}^2 + q)\right]^{1/2}}, \quad i = 1, 2, 3.$$

In this version of reference-body choice, the generalized singular approximation leads to the Maxwell–Garnett generalization [5], and Eq. (5) takes the form

$$\boldsymbol{\varepsilon}_\mathbf{e} = \left[(1 - d)\varepsilon_m \mathbf{I} + d\langle \boldsymbol{\kappa}_k \rangle\right] \cdot \left[(1 - d)\mathbf{I} + d\langle \boldsymbol{\lambda}_k \rangle\right]^{-1}. \tag{6}$$

Here the tensors related to a specific inclusion are introduced,

$$\boldsymbol{\lambda}_k = (\mathbf{I} - \mathbf{g}_k(\boldsymbol{\varepsilon}_k - \varepsilon_m \mathbf{I}))^{-1}, \quad \boldsymbol{\kappa}_k = \boldsymbol{\varepsilon}_k \boldsymbol{\lambda}_k, \quad k = \overline{1, N}.$$

The tensor $\boldsymbol{\lambda}_k$ has a clear physical meaning; it relates the field strength $\mathbf{E}_k$ within a single ellipsoidal inclusion and the applied uniform field $\mathbf{E}_m$ in an infinite matrix, $\mathbf{E}_k = \boldsymbol{\lambda}_k \mathbf{E}_m$ [11]. Then, to simplify the expressions, we omit the subscript k related to the inclusion number. The principal values of tensors $\boldsymbol{\lambda}$ and $\boldsymbol{\kappa}$ are calculated by the following formulas (ε'_j are the principal values of the tensor $\boldsymbol{\varepsilon}$):

$$\lambda'_j = \varepsilon_m(\varepsilon_m + L_j(\varepsilon'_j - \varepsilon_m))^{-1}, \quad \kappa'_j = \varepsilon'_j \lambda'_j, \quad j = 1, 2, 3. \tag{7}$$

The tensors $\boldsymbol{\lambda}$ and $\boldsymbol{\kappa}$ in Eq. (6) are averaged over all sample inclusions. In this case, this is averaging over all orientations and inclusion shapes. Under the assumption that the inclusion shape and orientation are independent, averaging is performed sequentially over inclusion orientations and shapes,

$$\langle \boldsymbol{\lambda} \rangle = \langle \langle \boldsymbol{\lambda} \rangle_o \rangle_f, \quad \langle \boldsymbol{\kappa} \rangle = \langle \langle \boldsymbol{\kappa} \rangle_o \rangle_f,$$

where $\langle \cdot \rangle_f$ is averaging over shapes and $\langle \cdot \rangle_o$ is averaging over the orientations of inclusions.

AVERAGING OVER INCLUSION ORIENTATIONS

Let the inclusion shape be fixed. We introduce the coordinate system xyz related to the composite sample, while each inclusion is related to the coordinate system $\xi\eta\zeta$ of principal axes of its ellipsoid. Then the inclusion orientation $g \equiv g(\psi, \theta, \varphi)$ in the system xyz (ψ, θ, φ are Euler angles) is the turn from xyz to $\xi\eta\zeta$. The volume fraction dV/V of crystallites whose orientations belong to the volume element of angular parameters $d^3\boldsymbol{\omega} = [\psi; \psi + d\psi] \otimes [\theta; \theta + d\theta] \otimes [\varphi; \varphi + d\varphi]$ is given by

$$dV/V = F(\psi, \theta, \varphi) \sin\theta \, d\psi \, d\theta \, d\varphi,$$

where $F(\psi, \theta, \varphi)$ is the inclusion-orientation distribution function (ODF) [13]. Tensors $\boldsymbol{\lambda}$, $\boldsymbol{\kappa}$ in the system xyz are averaged by the formulas

$$\langle \boldsymbol{\lambda} \rangle_o = \int\limits_{SO(3)} \boldsymbol{\lambda} F(g) dg, \quad \langle \boldsymbol{\kappa} \rangle_o = \int\limits_{SO(3)} \boldsymbol{\kappa} F(g) dg,$$

where the integral over the SO(3) group has the form

$$\int\limits_{SO(3)} (\cdot)\, dg \equiv \int\limits_0^{2\pi} \int\limits_0^{\pi} \int\limits_0^{2\pi} (\cdot) \sin\theta d\psi d\theta d\varphi.$$

Using rotation-group-representation theory, the following expressions for the orientation-averaged components of tensors $\boldsymbol{\lambda}$ and $\boldsymbol{\kappa}$ were obtained in the system xyz [9] (the numbering of subscripts $l, j = 1, 2, 3$ of tensor components in the system xyz implies the correspondence $x_1 \equiv x$, $x_2 \equiv y$, $x_3 \equiv z$):

$$\begin{aligned}
\langle \alpha_{jj} \rangle_o &= \frac{A}{3} + (-1)^{j+1} \sum_{s=-2}^{2} \tilde{\alpha}'_s \int\limits_{SO(3)} dg F(g) \Big[T^2_{-2,s}(g) + T^2_{2,s}(g) + (-1)^j \sqrt{2/3}\, T^2_{0,s}(g) \Big], \quad j = 1, 2; \\
\langle \alpha_{33} \rangle_o &= \frac{A}{3} + \sqrt{8/3} \sum_{s=-2}^{2} \tilde{\alpha}'_s \int\limits_{SO(3)} dg F(g) T^2_{0,s}(g), \\
\langle \alpha_{12} \rangle_o &= i \sum_{s=-2}^{2} \tilde{\alpha}'_s \int\limits_{SO(3)} dg F(g) \Big[T^2_{2,s}(g) - T^2_{-2,s}(g) \Big]; \\
\langle \alpha_{j3} \rangle_o &= (-i)^{j-1} \sum_{s=-2}^{2} \tilde{\alpha}'_s \int\limits_{SO(3)} dg\, F(g) \Big[T^2_{-1,s}(g) + (-1)^j T^2_{1,s}(g) \Big], \quad j = 1, 2,
\end{aligned} \tag{8}$$

where $A = \alpha'_1 + \alpha'_2 + \alpha'_3$; α_{lj}, α'_j, $\tilde{\alpha}'_m$ ($l, j = 1, 2, 3$, $m = -2, \ldots, 2$) are λ_{lj}, λ'_j, $\tilde{\lambda}'_m$ if $\langle \lambda_{lj} \rangle_o$ are calculated or κ_{lj}, κ'_j, $\tilde{\kappa}'_m$ if $\langle \kappa_{lj} \rangle_o$ are calculated.

The values of $\tilde{\lambda}'_m$, $\tilde{\kappa}'_m$, $m = -2, \ldots, 2$ are determined by the formulas

$$\begin{cases} \tilde{\lambda}'_{-2} = \tilde{\lambda}'_2 = (\lambda'_1 - \lambda'_2)/2, & \tilde{\lambda}'_0 = (2\lambda'_3 - \lambda'_1 - \lambda'_2)/\sqrt{6}, \quad \tilde{\lambda}'_{-1} = \tilde{\lambda}'_1 = 0, \\ \tilde{\kappa}'_{-2} = \tilde{\kappa}'_2 = (\kappa'_1 - \kappa'_2)/2, & \tilde{\kappa}'_0 = (2\kappa'_3 - \kappa'_1 - \kappa'_2)/\sqrt{6}, \quad \tilde{\kappa}'_{-1} = \tilde{\kappa}'_1 = 0; \end{cases} \tag{9}$$

$T^l_{ms}(g) \equiv T^l_{ms}(\psi, \theta, \varphi)$, $l = 0, 1, \ldots$; $m, s = \overline{-l, l}$ are the generalized spherical functions [14].

If the inclusion shape is random, expressions (8) should also be averaged over the inclusion shapes. Under the assumption that the inclusion orientation and shape are independent, expressions (8) after averaging over the inclusion shape take the form

$$\left\langle \langle \alpha_{jj} \rangle_o \right\rangle_f = \langle A \rangle_f / 3 + (-1)^{j+1} \sum_{s=-2}^{2} \langle \tilde{\alpha}'_s \rangle_f \int_{SO(3)} dg F(g) \left[T^2_{-2,s}(g) + T^2_{2,s}(g) + (-1)^j \sqrt{2/3}\, T^2_{0,s}(g) \right], \quad j = 1, 2,$$

$$\left\langle \langle \alpha_{33} \rangle_o \right\rangle_f = \langle A \rangle_f / 3 + \sqrt{8/3} \sum_{s=-2}^{2} \langle \tilde{\alpha}'_s \rangle_f \int_{SO(3)} dg\, F(g) T^2_{0,s}(g);$$

$$\left\langle \langle \alpha_{12} \rangle_o \right\rangle_f = i \sum_{s=-2}^{2} \langle \tilde{\alpha}'_s \rangle_f \int_{SO(3)} dg\, F(g) \left[T^2_{2,s}(g) - T^2_{-2,s}(g) \right]; \tag{10}$$

$$\left\langle \langle \alpha_{j3} \rangle_o \right\rangle_f = (-i)^{j-1} \sum_{s=-2}^{2} \langle \tilde{\alpha}'_s \rangle_f \int_{SO(3)} dg\, F(g) \left[T^2_{-1,s}(g) + (-1)^j T^2_{1,s}(g) \right], \quad j = 1, 2.$$

Formulas (10) are convenient for applications, since the ODF is often written as the Fourier series in generalized spherical functions [13]: $F(g) = \sum_{l=0}^{\infty} \sum_{m,n=-l}^{l} C^l_{mn} \overline{T^l_{mn}(g)}$. In this case, for the averaged components of tensors $\boldsymbol{\lambda}$ and $\boldsymbol{\kappa}$, we obtain expressions [10] containing Fourier coefficients of the distribution function $F(g)$ of only weight 2, i.e., $C^2_{m,n}$, $m, n = -2, \ldots, 2$ which can be experimentally determined by X-ray or neutron diffraction methods.

Let us consider in detail the specific distribution of inclusion orientations, i.e., the central normal distribution (CND) with one parameter β. The CND is a particular case of normal distributions over the SO(3) group, i.e., the limit distributions to which body orientation distributions tend during random rotational walks; it is often used in describing textures [13]. In the case of the CND, ODF expansion in generalized spherical functions is given by [13]

$$F(\beta, g) = \frac{1}{8\pi^2} \sum_{l=0}^{\infty} (2l+1) e^{-\beta^2 l(l+1)} \sum_{m=-l}^{l} \overline{T^l_{mm}(g)}. \tag{11}$$

The parameter β is related to the inclusion-orientation spread: $\langle \cos\theta \rangle = e^{-2\beta^2}$, $\langle \sin^2\theta \rangle = 2(1 - e^{-6\beta^2})/3$. In the case of the CND of inclusion orientations for components $\boldsymbol{\varepsilon}_e$ in the system xyz, we obtain

$$(\varepsilon_e)_{jj} = \frac{3\varepsilon_m + r[\langle K \rangle_f + (3\langle \kappa'_j \rangle_f - \langle K \rangle_f) e^{-6\beta^2}]}{3 + r[\langle D \rangle_f + (3\langle \lambda'_j \rangle_f - \langle D \rangle_f) e^{-6\beta^2}]}, \tag{12}$$

$$j = 1, 2, 3; \quad (\varepsilon_e)_{lj} = 0, \quad l \neq j,$$

where $D = \lambda'_1 + \lambda'_2 + \lambda'_3$, $K = \kappa'_1 + \kappa'_2 + \kappa'_3$.

AVERAGING OVER INCLUSION SHAPES

Let one semiaxis of all inclusions be fixed: $a_3 = c = fixe$, while two others randomly deviate from a certain average value equal to a, i.e., $\langle a_1 \rangle = \langle a_2 \rangle = a$. Then the random inclusion shape is determined by a random vector with components equal to the relative deviations e_1, e_2 of the semiaxes a_1, a_2 from their average values: $e_j = (a_j - a)/a$, $j = 1, 2$, therewith $\langle e_1 \rangle = \langle e_2 \rangle = 0$. Let the variances of e_1, e_2 be small: $\langle e_j{}^2 \rangle \equiv \sigma_j{}^2 \ll 1$, $j = 1, 2$, and e_1 and e_2 are independent; therefore, $\langle e_1 e_2 \rangle = 0$. Thus, the average shape of all inclusions is a spheroid with semiaxes a, a, c.

As seen from formulas (9) and (10), to average the components of tensors $\boldsymbol{\lambda}$ and $\boldsymbol{\kappa}$ in the system xyz over all inclusions, we should calculate the average values of the principal values of tensors $\boldsymbol{\lambda}$ and $\boldsymbol{\kappa}$ over the shape, i.e., $\langle \lambda'_j \rangle_f, \langle \kappa'_j \rangle_f$, $j = 1, 2, 3$. Since the effect of inclusion shape on λ'_j, κ'_j manifests itself via the geometrical factors of the ellipsoid L_1, L_2, L_3, we expand them in powers of e_1, e_2 to the 2nd order inclusive:

$$L_j(a_1, a_2, c) = L_j{}^0 + \Delta L_j,$$

$$\Delta L_j \approx A_{j1} e_1 + A_{j2} e_2 + B_{j1} e_1{}^2 + B_{j2} e_2{}^2 + C_j e_1 e_2, \tag{13}$$

$$j = 1, 2, 3,$$

$$L_j{}^0 = L_j(a, a, c), \quad A_{j1} = a \frac{\partial L_j(a, a, c)}{\partial a_1},$$

$$A_{j2} = a \frac{\partial L_j(a, a, c)}{\partial a_2},$$

$$B_{j1} = \frac{a^2}{2} \frac{\partial^2 L_j(a, a, c)}{\partial a_1{}^2}, \quad B_{j2} = \frac{a^2}{2} \frac{\partial^2 L_j(a, a, c)}{\partial a_2{}^2},$$

$$C_j = a^2 \frac{\partial^2 L_j(a, a, c)}{\partial a_1 \partial a_2}, \quad j = 1, 2, 3.$$

Calculating this set, we have

$$A_{11}=A_{22}=\frac{a^2c}{2}J_2-\frac{3}{2}a^4cJ_3,$$
$$A_{12}=A_{21}=\frac{a^2c}{2}(J_2-a^2J_3), \quad (14)$$
$$A_{31}=A_{32}=\frac{a^2c}{2}(\tilde{J}_1-a^2\tilde{J}_2),$$
$$B_{11}=B_{22}=\frac{15}{4}a^6cJ_4-\frac{9}{4}a^4cJ_3,$$
$$B_{12}=B_{21}=\frac{3}{4}a^4c(a^2J_4-J_3),$$
$$B_{31}=B_{32}=\frac{3}{4}a^4c(a^2\tilde{J}_3-\tilde{J}_2),$$

where

$$J_n=\int_0^\infty\frac{dq}{(a^2+q)^n(c^2+q)^{1/2}},$$
$$\tilde{J}_n=\int_0^\infty\frac{dq}{(a^2+q)^n(c^2+q)^{3/2}}.$$

Let us show the expressions for these integrals.

1. At $a>c$. The average shape is an oblate spheroid with the eccentricity $e=\sqrt{1-c^2/a^2}$.

$$\tilde{J}_1=\frac{2}{a^3e^2}\left((1-e^2)^{-1/2}-e^{-1}\arccos\sqrt{1-e^2}\right),$$
$$J_2=\frac{1}{a^3e^2}\left(e^{-1}\arccos\sqrt{1-e^2}-\sqrt{1-e^2}\right),$$
$$\tilde{J}_2=\frac{1}{a^5e^4}\left((3-e^2)(1-e^2)^{-1/2}-3e^{-1}\arccos\sqrt{1-e^2}\right),$$
$$J_3=\frac{1}{2a^5e^5}\left(\frac{3}{2}\arccos\sqrt{1-e^2}-\left(\frac{3}{2}e+e^3\right)\sqrt{1-e^2}\right),$$
$$J_4=\frac{1}{24a^7e^6}\left(\frac{15}{e}\arccos\sqrt{1-e^2}-(8e^4+10e^2+15)\sqrt{1-e^2}\right),$$
$$\tilde{J}_3=\frac{2}{a^7\sqrt{1-e^2}}-6J_4.$$

2. At $a<c$. The average shape is a prolate spheroid with the eccentricity $e=\sqrt{1-a^2/c^2}$.

$$\tilde{J}_1=\frac{2(1-e^2)^{3/2}}{a^3e^2}\left(-1+\frac{1}{2e}\ln\frac{1+e}{1-e}\right),$$
$$J_2=\frac{\sqrt{1-e^2}}{a^3e^2}\left(1-\frac{1-e^2}{2e}\ln\frac{1+e}{1-e}\right),$$
$$\tilde{J}_2=\frac{(1-e^2)^{3/2}}{a^5e^4}\left(3-2e^2-\frac{3}{2}\frac{1-e^2}{e}\ln\frac{1+e}{1-e}\right),$$
$$J_3=\frac{(1-e^2)^{5/2}}{4a^5e^6}\left(\frac{2}{(1-e^2)^2}-\frac{7}{1-e^2}+5+\frac{3}{2}e\ln\frac{1+e}{1-e}\right),$$
$$J_4=\frac{(1-e^2)^{7/2}}{24a^7e^8}\left(\frac{8}{(1-e^2)^3}-\frac{34}{(1-e^2)^2}+\frac{59}{1-e^2}-33-\frac{15}{2}e\ln\frac{1+e}{1-e}\right),$$
$$\tilde{J}_3=\frac{2\sqrt{1-e^2}}{a^7}-6J_4.$$

3. At $a=c$. The average shape is a sphere of radius c.

$$J_n=\tilde{J}_{n-1}=\frac{1}{(n-1/2)a^{2n-1}},\quad n=2,3,4.$$

Using set (13), we expand Eq. (7) in powers of e_1, e_2 to the 2nd order inclusive:

$$\lambda'_j\approx\lambda'^0_j[1+q_j(-A_{j1}-A_{j2})(e_1+e_2)+({q_j}^2{A_{j1}}^2-q_jB_{j1}){e_1}^2+({q_j}^2{A_{j2}}^2-q_jB_{j2}){e_2}^2+(2{q_j}^2A_{j1}A_{j2}-C_j)e_1e_2],\quad j=1,2,3, \quad (15)$$

$$\lambda'^0_j=\frac{\varepsilon_m}{\varepsilon_m+L_j^0(\varepsilon'_j-\varepsilon_m)},\quad q_j=\frac{\varepsilon'_j-\varepsilon_m}{\varepsilon_m+L_j^0(\varepsilon'_j-\varepsilon_m)}. \quad (16)$$

Averaging Eq. (15) over the shape, taking into account Eq. (7), we have

$$\langle\lambda'_j\rangle_f\approx\lambda'^0_j[1+z_j{\sigma_1}^2+y_j{\sigma_2}^2],\quad \langle\kappa'_j\rangle_f=\varepsilon'_j\langle\lambda'_j\rangle_f,\quad j=1,2,3, \quad (17)$$

$$z_j={q_j}^2{A_{j1}}^2-q_jB_{j1},\quad y_j={q_j}^2{A_{j2}}^2-q_jB_{j2}. \quad (18)$$

SIMULATION RESULTS FOR THE FREQUENCY DIELECTRIC CHARACTERISTICS OF POROUS SILICON AND DISCUSSION

Formulas (12), and (16)–(18) were used to calculate the frequency dielectric characteristics of porous silicon with fibrous or layered structures in the system *xyz* in the frequency range of 10^3–10^8 Hz. A formally continuous medium in such a material is silicon; however, due to its small volume fraction in the material, it was considered as inclusions, and air was considered as the matrix. Porous silicon with the fibrous structure was modeled by inclusions of random ellipsoidal shape with a small spread around the average strongly prolate spheroidal shape. The material with the layered structure was modeled by inclusions with a small deviation from the average strongly oblate spheroidal shape. The inclusion orientation was considered to be distributed according to the CND law with the ODF in the form of Eq. (11) at various β. In the absence of inclusion-orientation spread, inclusion semiaxes a_1, a_2, a_3 are parallel to the x, y, z axes, respectively. Bonding bridges between fibers or layers in the material were disregarded; this requires a more complex model.

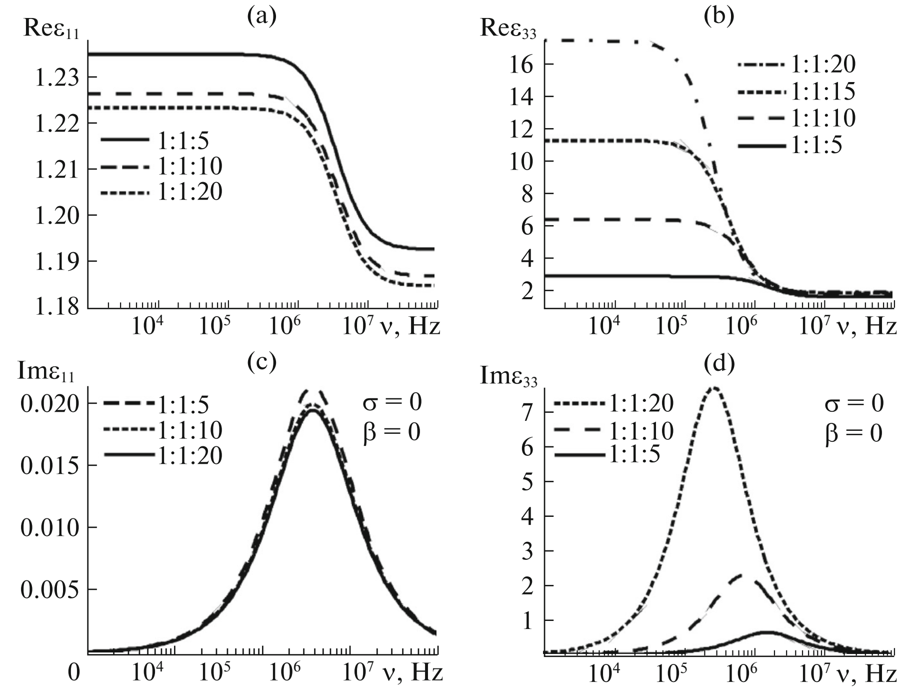

Fig. 1. Frequency dependences of the (a) real and (c) imaginary parts of the component $(\varepsilon_e)_{11}$ and (b) real and (d) imaginary parts of the component $(\varepsilon_e)_{33}$ of the model of porous silicon with spheroidal prolate inclusions at various ratios of semiaxes *a*:*b*:*c*. Inclusion orientation and shape spreads are lacking; the inclusion volume fraction is 0.1.

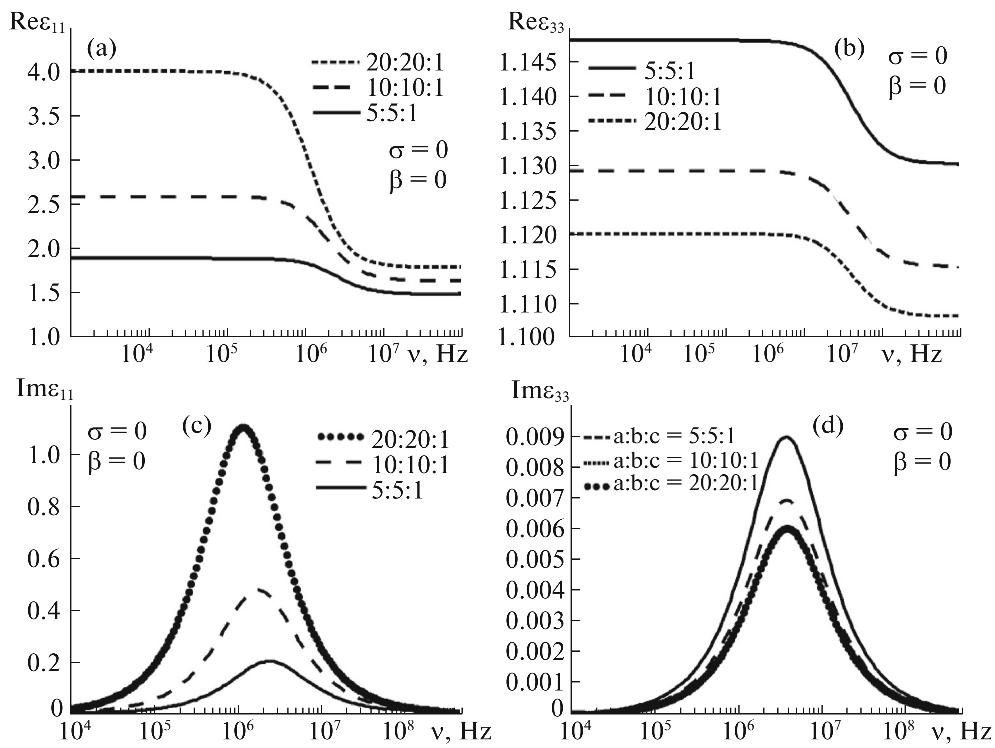

Fig. 2. Frequency dependences of the (a) real and (c) imaginary parts of the component $(\varepsilon_e)_{11}$ and (b) real and (d) imaginary parts of the component $(\varepsilon_e)_{33}$ of the model of porous silicon with spheroidal oblate inclusions at various ratios of semiaxes *a*:*b*:*c*. Inclusion orientation and shape spreads are lacking; the inclusion volume fraction is 0.1.

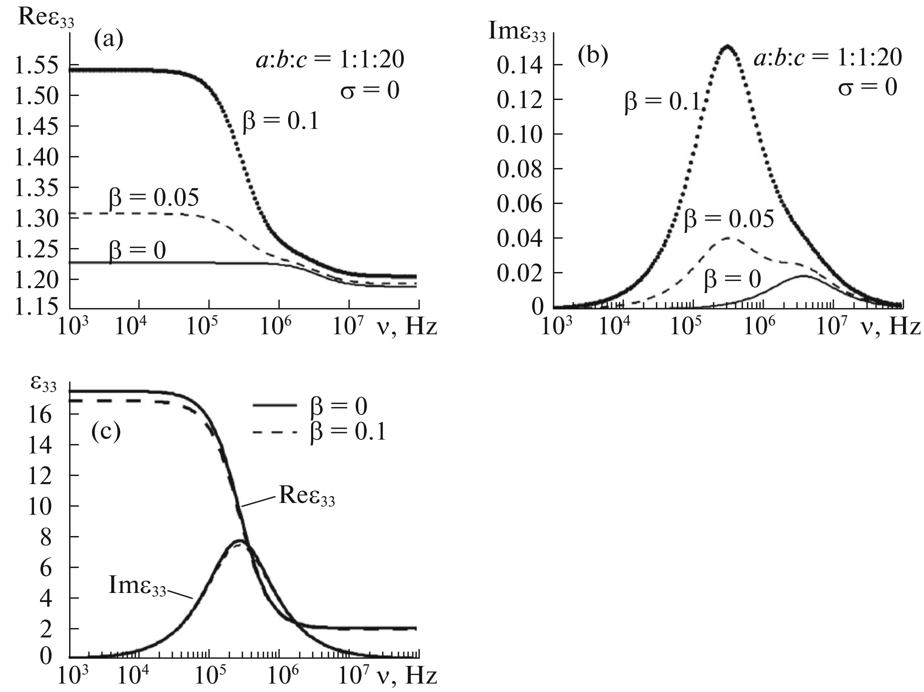

Fig. 3. Frequency dependences of the (a) real and (b) imaginary parts of the component $(\varepsilon_e)_{11}$ and (c) real and imaginary parts of the component $(\varepsilon_e)_{33}$ of the models of porous silicon with spheroidal prolate inclusions with a semiaxis ratio of 1:1:20 at various inclusion-orientation spreads. The orientation distribution is CND-type. Shape spread is lacking. The inclusion volume fraction is 0.1.

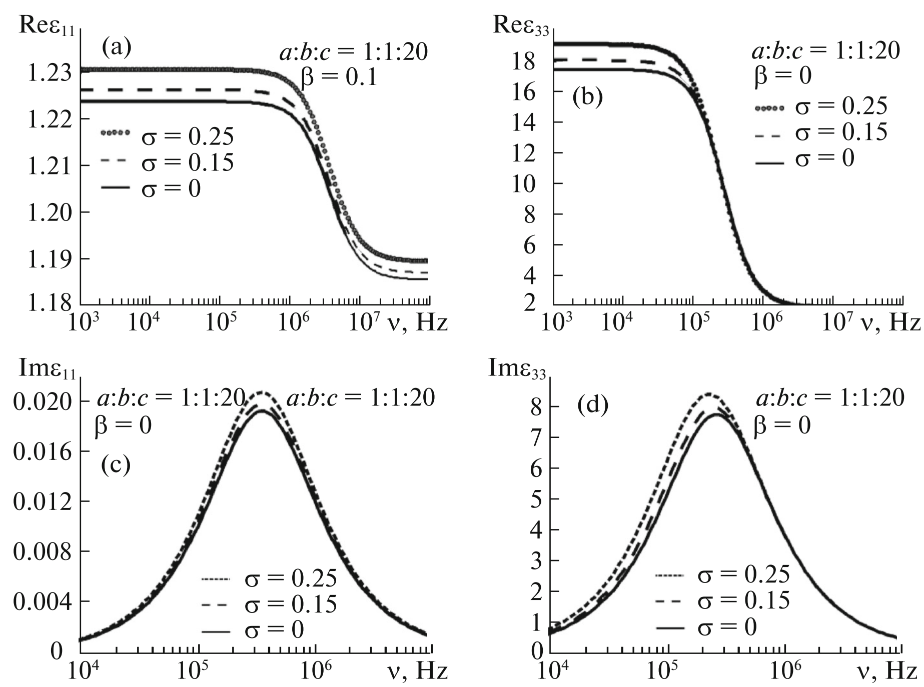

Fig. 4. Frequency dependences of the (a) real and (c) imaginary parts of the component $(\varepsilon_e)_{11}$ and (b) real and (d) imaginary parts of the component $(\varepsilon_e)_{33}$ of the model of porous silicon with prolate inclusions with an average semiaxis ratio of 1:1:20 at various inclusion-shape spreads $\sigma_1 = \sigma_2 = \sigma$. The orientation spread is lacking; the inclusion volume fraction is 0.1.

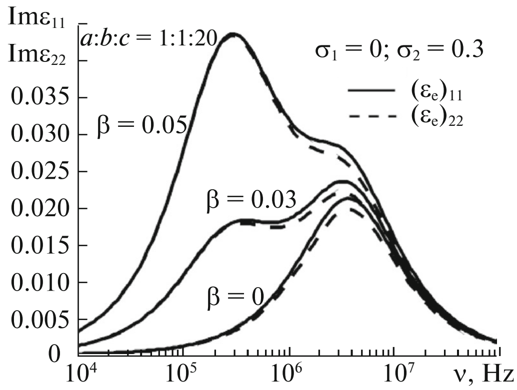

Fig. 5. Frequency dependences of the imaginary part of components $(\varepsilon_e)_{11}$ (solid curves) and $(\varepsilon_e)_{22}$ (dashed curves) of the model of porous silicon with random prolate inclusions with an average semiaxis ratio of 1:1:20 at various inclusion-orientation spreads β. The orientation distribution is CND-type; the inclusion-semiaxis spreads are $\sigma_1 = 0$, $\sigma_2 = 0.3$; the inclusion volume fraction is 0.1.

The objective of the simulation is to study the effect of the average inclusion shape, orientation and shape spreads on the dielectric characteristics of porous silicon. The dependence of the silicon permittivity on the electromagnetic-field frequency at low frequencies is written as $\varepsilon(\omega) = \varepsilon_s + i\,4\pi\sigma_s/\omega$, where $\sigma_s = 0.435 \times 10^{-3}\ \Omega^{-1}\ \text{m}^{-1}$ is the static conductivity of silicon and $\varepsilon_s = 11.7$ is the static permittivity [15]. Some results of calculations are shown in Figs. 1–5.

The frequency dielectric characteristics of porous silicon (Figs. 1 and 2) at a fixed inclusion shape and orientation show that the characteristics of the principal components $(\varepsilon_e)_{11}$ and $(\varepsilon_e)_{33}$ of the tensor $\boldsymbol{\varepsilon}_e$ differ significantly from each other. For porous silicon with the fibrous structure (see Fig. 1), the real and imaginary parts of component $(\varepsilon_e)_{33}$ significantly exceed the corresponding parts of component $(\varepsilon_e)_{11}$ in magnitude. In turn, $\mathrm{Re}(\varepsilon_e)_{33}$ (Fig. 1b) and $\mathrm{Im}(\varepsilon_e)_{33}$ (Fig. 1d) depend on the ratio of the semiaxes *a*:*b*:*c*. They increase with the ratio *c*:*a*. The real (Fig. 1a) and imaginary (Fig. 1c) parts of the component $(\varepsilon_e)_{11}$ also depend on the ratio *c*:*a*; however, this dependence is opposite. The frequency characteristics of $\mathrm{Im}(\varepsilon_e)_{11}$ and $\mathrm{Im}(\varepsilon_e)_{33}$ have maxima whose values and positions depend on the ratio *c*:*a*. For the model of porous silicon with the layered structure (see Fig. 2), similar dependences of $(\varepsilon_e)_{11}$ and $(\varepsilon_e)_{33}$ on the ratio *c*:*a* are observed; however, $(\varepsilon_e)_{11}$ has larger values than $(\varepsilon_e)_{33}$ in this case.

The dependences (Fig. 3) for the model of porous silicon with the fibrous structure show that the appearance of orientation spread causes the mixing of "pure" components of the tensor $\boldsymbol{\varepsilon}_e$, corresponding to the case of strictly oriented inclusions. For example, a maximum corresponding to $\mathrm{Im}(\varepsilon_e)_{33}$ appears in the dependence of $\mathrm{Im}(\varepsilon_e)_{11}$ and grows as the inclusion-orientation spread β increases (Fig. 3b). The change in the dependences of $\mathrm{Re}(\varepsilon_e)_{33}$ and $\mathrm{Im}(\varepsilon_e)_{33}$ with increasing β is much less distinct (Fig. 3c). This is explained by the fact that "pure" components $\mathrm{Re}(\varepsilon_e)_{33}$ and $\mathrm{Im}(\varepsilon_e)_{33}$ far exceed $\mathrm{Re}(\varepsilon_e)_{11}$ and $\mathrm{Im}(\varepsilon_e)_{11}$ in magnitude. As shape variance appears (see Fig. 4), both parts of components $(\varepsilon_e)_{11}$ and $(\varepsilon_e)_{33}$ of the model of porous silicon with the fibrous structure slightly increase, and the maxima of the imaginary part slightly shift, which is especially pronounced for $\mathrm{Im}(\varepsilon_e)_{33}$ (Fig. 4d). Similar changes are observed in the simulation of the systems with the layered structure as well.

We note that components $(\varepsilon_e)_{11}$ and $(\varepsilon_e)_{22}$ have identical characteristics in all cases (see Figs. 1–4). First, this due to the fact that the average inclusion shape is spheroidal; second, the coordinate axes *x*, *y*, *z* are equivalent for CND-type orientation distributions (11); third, the root-mean-square deviations of the inclusion semiaxes were set equal, $\sigma_1 = \sigma_2 = \sigma$ in all cases.

The frequency dependences of $\mathrm{Im}(\varepsilon_e)_{11}$ and $\mathrm{Im}(\varepsilon_e)_{22}$ for the case $\sigma_1 = 0 \neq \sigma_2 = 0.3$ (see Fig. 5) slightly differ from each other; therewith $\mathrm{Im}(\varepsilon_e)_{11} > \mathrm{Im}(\varepsilon_e)_{22}$, despite the fact that the semiaxis a_1 is fixed, while the semiaxis a_2 exhibits random variation. This phenomenon of the pronounced effect of random variation of the semiaxis a_2 on $\mathrm{Im}(\varepsilon_e)_{11}$ has a simple physical interpretation: let $\sigma_1 = 0$, $\sigma_2 > 0$, $a_1 = a$, $\langle a_2 \rangle = a$. Restricting the expansion (13) of the geometrical factors to second-order terms, we obtain an even distribution of the relative deviation e_2 of the semiaxis a_2; therefore, the volume fraction of inclusions with semiaxis $a_2 = a + \delta$ will be equal to the volume fraction of inclusions with $a_2 = a - \delta$ at any admissible $\delta > 0$. Let us compare the ratios of the larger of the semiaxis a_1 and a_2 to the smaller one in the first and second cases,

$$\left(\frac{a_2}{a_1}\right)_1 = \frac{a+\delta}{a} < \left(\frac{a_1}{a_2}\right)_2 = \frac{a}{a-\delta},$$

i.e., the relative "prolateness" of inclusions toward the semiaxis a_1 in the second case is larger than toward the semiaxis a_2 in the first case; the relative "oblateness" toward the semiaxis a_1 in the first case is less than toward the semiaxis a_2 in the second case; in combination, these factors cause higher values of $\mathrm{Im}(\varepsilon_e)_{11}$.

Thus, the effective permittivity tensor $\boldsymbol{\varepsilon}_e$ of a heterogeneous textured matrix-type material with inclusions of random ellipsoidal shape is calculated by formula (6). The average components of tensors $\boldsymbol{\lambda}$ and $\boldsymbol{\kappa}$ in the system *xyz* related to the material texture at random distribution of inclusion orientations are determined by formulas (10), (14), (16)–(18). In the case of central normal distribution of the SO(3) group, the $\boldsymbol{\varepsilon}_e$ components are calculated by formulas (12).

The method proposed in this paper can be used to predict the dielectric properties of heterogeneous systems in an alternating electromagnetic field, which can find application in the development of materials with desirable physical properties and in the development of methods for analyzing the results of dielectric spectroscopy, e.g., in geophysics and related fields. The model of a heterogeneous textured material, constructed in this paper, can be used as a basis for the development of sophisticated models reflecting the structure of studied materials in more detail.

An important advantage of the developed method is its low computing resource use from the viewpoint of time and memory size.

However, it should be noted that this method cannot be applied to the study of the optical properties of composites with randomly shaped metal inclusions, since the term with respect to which the expansion is performed in formula (15) becomes unacceptably large near the plasmon resonance.

ACKNOWLEDGMENTS

This study was supported by the Russian Foundation for Basic Research, projects nos. 13-08-00672-a and 14-08-00654-a).

REFERENCES

1. A. G. Fokin, Sov. Tech. Phys. **16**, 849 (1971).
2. A. G. Fokin, Sov. Tech. Phys. **18**, 44 (1973).
3. T. D. Shermergor, *Theory of Elasticity of Micro-Inhomogeneous Media* (Nauka, Moscow, 1977) [in Russian].
4. V. B. Yakovlev, V. V. Bardushkin, I. V. Lavrov, et al., Izv. Vyssh. Uchebn. Zaved., Elektron., No. 3, 7 (2013).
5. V. I. Kolesnikov, V. B. Yakovlev, V. V. Bardushkin, I. V. Lavrov, A. P. Sychev, and E. N. Yakovleva, Dokl. Phys. **58**, 379 (2013).
6. S. Giordano, Int. J. Eng. Sci. **43**, 1033 (2005).
7. S. Giordano, J. Electrost. **64**, 655 (2006).
8. E. N. Ivanov and I. V. Lavrov, Oboron. Kompleks Nauch.-Tekh. Progressu Rossii., No. 1, 73 (2007).
9. I. V. Lavrov, Ekol. Vestn. Nauch. Tsentrov Chernomor. Ekon. Sotrudn., No. 1, 52 (2009).
10. I. Lavrov, *Dielectric and Conductive Properties of Inhomogeneous Media with Texture* (LAP Lambert Academic, Saarbrücken, 2011) [in Russian].
11. C. Bohren and D. Huffman, *Absorption and Scattering of Light by Small Particles* (Wiley, New York, 1998; Mir, Moscow, 1986).
12. I. E. Protsenko, O. A. Zaimidoroga, and V. N. Samoilov, J. Opt. A: Pure Appl. Opt. **9**, 363 (2007).
13. M. V. Borovkov and T. I. Savyolova, *Normal Distributions on SO(3)* (Mosk. Inzhen. Fiz. Inst., Moscow, 2002) [in Russian].
14. I. M. Gelfand, R. A. Minlos, and Z. Ya. Shapiro, *Representations of the Rotation and Lorentz Groups and their Applications* (Pergamon, Oxford, 1963; Fizmatgiz, Moscow, 1958).
15. *Physical Values, the Handbook,* Ed. by I. S. Grigor'ev and E. Z. Meilikhov (Energoatomizdat, Moscow, 1991) [in Russian].

Translated by A. Kazantsev